MATERIALS PHYSICS AND MECHANICS RESEARCH ARTICLE

Submitted: October 18, 2025 **Revised: November 13, 2025** **Accepted: November 24, 2025**

Study of optical resistance of a bulk β-Ga_2O_3 crystal

D.I. Panov, N.A. Balabanov, M.M. Sergeev, V.A. Spiridonov ✉, D.A. Bauman, A.E. Romanov

ITMO University, St. Petersburg, Russia

✉ vladspiridonov@itmo.ru

ABSTRACT

The optical resistance and geometric parameters of the damaged region under the action of laser radiation on bulk β-Ga_2O_3 crystal were studied and calculated depending on the power and frequency of laser irradiation. The sample of the crystal for the study was grown by the Czochralski method and prepared by method of cleaving along the (100) plane. The optical resistance was calculated by the Liu method using the laser irradiation and ablation parameters. The experiment determined the threshold for laser damage under pulses of 1030 nm wavelength and 224 fs duration; with a beam spot size of 9.6 μm. The threshold energy density varied from 25.99 to 16.29 J/cm^2 with pulse numbers varying from 1 to 20,000. The threshold power density of incident radiation ranged from 11.6 to 7.3 GW/cm^2.

KEYWORDS

gallium oxide • laser • optical resistance • Liu's method • laser ablation • laser radiation

Funding. *This work has been supported by the grant of the Russian Science Foundation, RSF 24-12-00229.*

Citation: Panov DI, Balabanov NA, Sergeev MM, Spiridonov VA, Bauman DA, Romanov AE. Study of optical resistance of a bulk β-Ga_2O_3 crystal. *Materials Physics and Mechanics*. 2026;54(1): 17–23. http://dx.doi.org/10.18149/MPM.5412026_3

Introduction

Beta-gallium oxide (β-Ga_2O_3) has emerged as a leading ultra-wide bandgap (UWBG) semiconductor, with a direct bandgap of ~ 4.8 eV, surpassing the performance limits of conventional materials like SiC and GaN [1–5]. Its exceptional properties including a high critical electric field (8 MV/cm^{-1}), excellent thermal stability, and the availability of high-quality substrates make it ideal for next-generation power devices, deep-ultraviolet (UV) photodetectors, and radiation-hardened applications [6–9].

Despite significant progress in understanding the electrical [10–14] and structural properties [14–20] of β-Ga_2O_3, critical challenges still remain in optimizing its performance and reliability for practical applications. One of the key issues is the material's response to various forms of radiation and environmental stress, particularly in optoelectronic applications where the material may be subjected to intense optical irradiation.

The beta phase of gallium oxide belongs to the monoclinic system, spatial group C2/m [21] with lattice parameters a = 12.214 Å, b = 3.0371 Å, c = 5.7981 Å, β = 103.83°. The unit cell of the crystal has three different oxygen positions, designated as O(1), O(2) and O(3), and two gallium positions, Ga(1) and Ga(2). Nodes O(1) and O(3) have the smallest coordination number 3, which leads to weak interplanar connections in planes (100) and (001) [22,23]. Due to the peculiarities of the crystal lattice, gallium oxide is an anisotropic material. It has been experimentally shown that a number of characteristics

(for example, thermal conductivity or electron mobility) have better values along the [010] direction [22–24]. However, mechanical processing is difficult due to fragility and mechanical defects of the material in the plane (010). As a result, other processing methods for β-Ga_2O_3 are being studied, including laser scribing [25–28]. Yoo J.H. et al. [29] studied the optical resistance of bulk gallium oxide, but these samples were doped with Sn, which makes its own adjustments to the optical resistance when compared with undoped samples. The paper presents the results of determining the optical resistance of β-Ga_2O_3 surface under the action of femtosecond laser pulses of the near-IR spectrum depending on the number of pulses and their repetition frequency from 10 to 201 kHz.

Materials and Methods

The sample of bulk crystal for studying the optical resistance of β-Ga_2O_3 was grown by Czochralski method using the NIKA-3 growth unit. The crystal growing process is described in detail in the paper [30]. The sample was prepared by method of chipping the bulk β-Ga_2O_3 crystal along the cleavage plane (100). The ablation of the material was performed on an experimental setup equipped with an ANTAUS-20W Yb-fiber femtosecond laser (Avesta) and a 3D coordinate moving system based on DDSM50 and MTS50M-Z8 translators (Thorlabs). For investigation the laser beam with Gaussian intensity profile, factor $M^2 < 1.1$, maximum average optical power $P_{max} = 17.5$ W at the pulse repetition frequency of 1 MHz, pulse duration of 224 fs, output beam diameter of 2.0 mm, and quasi-monochromatic wavelength 1030 nm, which transparent to β-Ga_2O_3, was used [1]. In the experiment, the laser beam was focused using a 40X, NA 0.60 objective lens into a spot with a diameter of 9.6 μm on the surface of the sample, while the latter was rigidly fixed on the coordinate table. Ablated areas were formed at the optical power in the range from 0.06 to 0.19 P_{max}, fixed exposure time of 0.1 s and different repetition pulse frequency: $201 \cdot 10^3$, $2 \cdot 10^3$, 200 and 10 Hz, respectively. As a result, the pulses number and time between its were variated as follows: 20,000 pulses every 5 μs, 200 pulses every 0.5 ms, 20 pulses every 5 ms and single pulse. Gentec Solo PE-2 M (Lake Oswego) optical power meters equipped with UP19K-110F-H9 pyroelectric power detector (Lake Oswego) used for registration of incident laser power. The uncertainty of the power meter calibration was $dP = \pm 2.5$ %.

Results and Discussion

To determine the optical resistance of the β-Ga_2O_3 sample, a series of experiments with ablated areas formation by different number pulses with a laser beam power in the range from 1.05 to 3.33 W. Figure 1 shows an optical microscope image of the sample after laser ablation. By analyzing the images obtained using a scanning electron microscope (Fig. 2), the diameters of the ablation crater were measured depending on the frequency and power of laser ablation.

It's observed from Table 1 that the value of the diameters of crater has a stepwise increase depending on a laser power. Thus, laser ablation can be quantitatively characterized by the crater diameter, which is necessary for calculating the optical resistance of the β-Ga_2O_3.

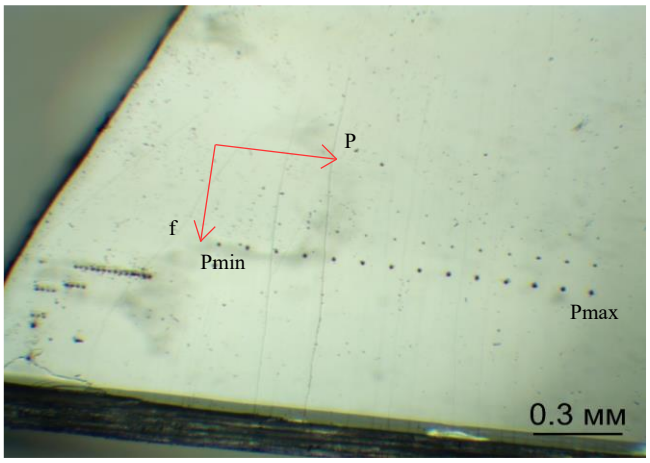

Fig. 1. An optical microscope image of β-Ga_2O_3 after laser ablation on a scale of 0.3 mm, with arrows indicating an increase in repetition rate (*f*) and optical power of laser beam (*P*)

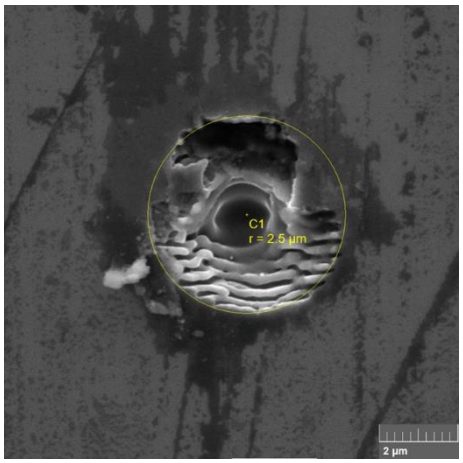

Fig. 2. An example of measuring the diameter of an ablation crater using a scanning electron microscope

Table 1. Diameter of ablated areas of sample surface in microns with error δD = ± 0.1 um

Number of pulses	Average optical power *P*, W													
	1.05	**1.22**	**1.40**	**1.57**	**1.75**	**1.92**	**2.10**	**2.27**	**2.45**	**2.62**	**2.80**	**2.97**	**3.15**	**3.32**
20,000	5.4	5.5	5.5	5.5	5.7	5.7	6.5	8.1	8.2	8.3	8.3	8.5	8.5	9.3
200	2.5	4.2	5.0	5.3	5.5	5.5	5.7	5.9	6.0	7.5	7.6	7.7	8.0	8.1
20	2.0	2.4	2.4	2.4	4.0	4.5	4.9	5.0	5.0	5.1	5.2	5.0	5.9	6.0
1	1.5	1.5	1.6	1.7	1.8	1.6	1.5	3.5	4.2	4.3	4.5	4.5	4.5	4.4

Calculation of the optical resistance

The optical resistance of the β-Ga_2O_3 surface was determined by measuring the diameter of the craters *D* formed as a result of laser ablation at different pulse energies *E* using the Lui method [31]. Depending on the diameter of the wells squared from the energy of the impulses at which they were formed, a linear regression was given by the expression:

$$D^2(E) = 2\omega_0^2 \ln(E/E_{th}), \quad (1)$$

where ω_0 is the radius of the laser spot determined by the intensity drop on e^{-2}, which formed the crater. The energy in the pulse was calculated from the average power of incident radiation *P*, measured at the pulse repetition frequency *f* = 20 kHz, as:

$$E = P/f. \quad (2)$$

According to Eq. (1), the graphical dependence $D^2(E/E_{th})$ was plotted on a logarithmic scale along the abscissa axis. In this case, the point of intersection of the linear regression with the abscissa axis determined the pulse energy E_{th}, at which the formation of the well began, and the slope of the line corresponded to the radius of the laser spot:

$$\omega_0 = [-b/(2E_{th})\cdot N_{ph}]^{0.5}, \quad (3)$$

where N_{ph} is the value of multiphoton absorption, *b* is the linear regression constant written as a function $y = kx + b$. This function was plotted based on experimental data by least squares approximation (Fig. 3). For all points, the exposure duration was 0.1 seconds. 20,000 pulses corresponded to a frequency of 201 kHz, 200 pulses corresponded to 2.01 kHz, 20 pulses corresponded to a frequency of 201 Hz and 1 pulse at 10 Hz.

The value of N_{ph} was determined as the ratio of the energy of the bandgap of the material E_g to the photon energy E_{ph} and characterized the cross-section of multiphoton absorption, i.e. the region of the Gaussian laser beam where the energy density provided N_{ph}-photon absorption of incident radiation. In our case, at E_g = 4 eV and E_{ph} = 1.2 eV (the energy of a photon with a wavelength of 1030 nm), the value of N_{ph} = 4.

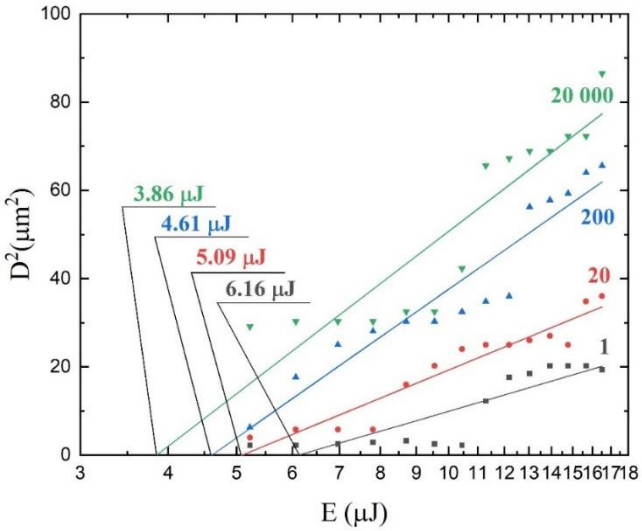

Fig. 3. Dependence of the square of the sublimation diameter on the pulse energy of the different pulses in the irradiated region: 1, 20, 200 and 20,000 pulses

Optical resistance of the sample was characterized by the energy density at which surface ablation began, and was expressed as follows:

$$F_{th} = E_{th}/(\pi\omega_0^2). \quad (3)$$

The constants of the linear regression, as well as the values of the laser spot radius and threshold energy density of the material are shown in Table 2. From the data provided, it can be seen that the threshold energy of E_{th} was maximum when exposed to a single pulse, equal to 6.16 μJ and decreased almost twice – to 3.86 μJ – with an increase in the number of pulses to 20,000. The radius of the laser spot did not depend on the number of pulses and was supposed to be 7.7 μm for all irradiation modes. An increase in the radius of the laser beam according to the computational data under the influence of 200 and 20,000 pulses indicated that the size of the ablative crater became larger than the laser spot due to spalling ablation. In this case, part of the material outside the irradiated zone was broken off and removed, thereby increasing the diameter of the ablation zone from 15.4 to 24.4 μm.

Table 2. Linear regression constants, threshold pulse energy, beam radius, threshold energy and power densities for optical resistance

Number of pulses/ repetition rate	*b*	*k*	E_{th}, μJ	ω_0, μm	F_{th}, J/cm²	W_{th}, W/cm²
1 / 10 Hz	-46.47 ± 5.96	65.76 ± 5.83	6.16	7.77	25.99 ± 4.21	$11.6 \cdot 10^9$
20 / 201 Hz	-36.81 ± 7.60	46.75 ± 7.43	5.09	7.61	21.48 ± 1.33	$9.6 \cdot 10^9$
200 / 2,01 kHz	-74.09 ± 10.64	111.68 ± 10.41	4.61	11.34	19.45 ± 3.35	$8.7 \cdot 10^9$
20,000 / 201 kHz	-71.54 ± 16.04	122.23 ± 15.69	3.86	12.18	16.29 ± 4.22	$7.3 \cdot 10^9$

The measurement error was estimated considering linear regression, the accuracy of measuring the diameter of the wells and the incident radiation power, for which an expression of the following form was used:

$$dF = F_{th}\sqrt{\left(\frac{dk}{k}\right)^2 + \left(\frac{db}{b}\right)^2 + \frac{1}{14}\sum_{i=1}^{14}\left(\frac{\delta D}{D_i}\right)^2 + \delta P^2}. \quad (4)$$

As a result, firstly, the average measurement error ranged from 16.4 % when exposed to 1 pulse to 26 % after exposure to 20,000 pulses. Measurement error can be reduced by recording not one, but several series of wells under the same laser exposure regimes. Secondly, the minimum error under the same other irradiation conditions was for the effect of a single pulse. Thirdly, ablation of the β-Ga_2O_3 surface under the influence of high-power near-infrared laser pulses occurred due to multiphoton absorption, which was random, unstable and contributed to a high measurement error. Reducing the wavelength to visible and near-UV radiation would also reduce measurement error.

From the above data of the threshold energy density F_{th}, it can be noted that its value decreased by 37 % with an increase in the number of pulses from 1 to 20,000 (Table 2). This result was typical for any materials in the transition from single-pulse to multi-pulse action. With each subsequent pulse, the fatigue of the material accumulated in the form of an increase in the concentration of local defects in the crystal lattice

Conclusions

Experiments on the effects of laser irradiation were carried out on samples of bulk crystals of gallium oxide grown using the Czochralski method and prepared by chipping along the cleavage plane. During the analysis of the laser ablation geometric parameters and calculations, the optical resistance of β-Ga_2O_3 was determined. The threshold energy density varied from 25.99 to 16.29 J/cm² with pulse numbers varying from 1 to 20,000 at a wavelength of 1030 nm and a pulse duration of 224 fs. The threshold power density of incident radiation ranged from 11.6 to 7.3 GW/cm².

CRediT authorship contribution statement

Dmitrii I. Panov: writing – review & editing, writing – original draft, conceptualization, data curation; **Nikita A. Balabanov**: writing – original draft, conceptualization, investigation; **Maxim M. Sergeev**: writing – review & editing, conceptualization, investigation; **Vladislav A. Spiridonov**: writing – review & editing, investigation ; **Dmitrii A. Bauman**: writing – review & editing; **Alexey E. Romanov**: writing – review & editing, supervision

Conflict of interest

The authors declare that they have no conflict of interest.

References

1. Spencer JA, Mock AL, Jacobs AG, Schubert M, Zhang Y, Tadjer MJ. A review of band structure and material properties of transparent conducting and semiconducting oxides: Ga_2O_3, Al_2O_3, In_2O_3, ZnO, SnO_2, CdO, NiO, CuO, and Sc_2O_3. *Applied Physics Reviews.* 2022;9(1): 011315.

2. Tsao JY, Chowdhury S, Hollis MA, Jena D, Johnson NM, Jones KA, Kaplar RJ, Rajan S, Van de Walle CG, Bellotti E, Chua CL, Collazo R, Coltrin ME, Cooper JA, Evans KR, Graham S, Grotjohn TA, Heller ER, Higashiwaki M, Islam MS, Juodawlkis PW, Khan MA, Koehler AD, Leach JH, Mishra UK, Nemanich RJ, Pilawa-Podgurski RCN, Shealy JB, Sitar Z, Tadjer MJ, Witulski AF, Wraback M, Simmons JA. Ultrawide-bandgap semiconductors: Research opportunities and challenges. *Advanced Electronic Materials.* 2018;4(1): 1600501.
3. Wong MH, Bierwagen O, Kaplar RJ, Umezawa H. Ultrawide-bandgap semiconductors: An overview. *Journal of Materials Research.* 2021;36: 4601–4615.
4. Woo K, Bian Z, Noshin M, Martinez RP, Malakoutian M, Shankar B, Chowdhury S. From wide to ultrawide bandgap semiconductors for high power and high frequency electronic devices. *Journal of Physics: Materials.* 2024;7(2): 022003.
5. Feng T, Zhou H, Cheng Z, Larkin LS, Neupane MR. A critical review of thermal boundary conductance across wide and ultrawide bandgap semiconductor interfaces. *ACS Applied Materials & Interfaces.* 2023;15(25): 29655–29673.
6. Dahiya S, Kaur D, Ghosh A, Kumar M. A strategic review on gallium oxide based power electronics: Recent progress and future prospects. *Materials Today Communications.* 2022;33: 104244.
7. Pearton SJ, Yang J, Cary PH, Ren F, Kim J, Tadjer MJ, Mastro MA. A review of Ga_2O_3 materials, processing, and devices. *Applied Physics Reviews.* 2018;5(1): 011301.
8. Petrenko AA, Kovach YaN, Bauman DA, Odnoblyudov MA, Bougrov VE, Romanov AE. Current state of Ga_2O_3-based electronic and optoelectronic devices. Brief review. *Reviews on Advanced Materials and Technologies.* 2021;3(2): 1–26.
9. Galazka Z. β-Ga_2O_3 for wide-bandgap electronics and optoelectronics. *Semiconductor Science and Technology.* 2018;33(11): 113001.
10. Singh R, Lenka TR, Panda DK, Velpula RT, Jain B, Bui HQT, Nguyen HPT. The dawn of Ga_2O_3 HEMTs for high power electronics—A review. *Materials Science in Semiconductor Processing.* 2020;119: 105216.
11. Wang X, Chang X, Wang P, Yang X, Yuan L. Research progress and prospect of the bulk single crystal growth of β-Ga_2O_3: From 1964 to 2024. *Crystal Research and Technology.* 2025;60(6): 2400255.
12. He Y, Zhao F, Huang B, Zhang T, Zhu H. A review of β-Ga_2O_3 power diodes. *Materials.* 2024;17(8): 1870.
13. Pearton SJ, Ren F, Polyakov AY, Haque A, Labed M, Rim YS. Status of Ga_2O_3 for power device and UV photodetector applications. *Applied Physics Reviews.* 2025;12(3): 031336.
14. He X, Wang M, Meng J, Hu J, Jiang Y. The effect of vacancy defects on the electronic properties of β-Ga_2O_3. *Computational Materials Science.* 2022;215: 111777.
15. Galazka Z. Growth of bulk β-Ga_2O_3 single crystals by the Czochralski method. *Journal of Applied Physics.* 2022;131(3): 031103.
16. Bauman DA, Panov DYu, Spiridonov VA, Kremleva AV, Asach AV, Tambulatova EV, Sakharov AV, Romanov AE. High quality β-Ga_2O_3 bulk crystals, grown by edge-defined film-fed growth method: Growth features, structural and thermal properties. *Journal of Vacuum Science & Technology A.* 2023;41(5): 053203.
17. Yao Y, Hirano K, Sugawara Y, Sasaki K, Kuramata A, Ishikawa Y. Observation of dislocations in thick β-Ga_2O_3 single-crystal substrates using Borrmann effect synchrotron X-ray topography. *APL Materials.* 2022;10(5): 051101.
18. Labed M, Sengouga N, Prasad CV, Henini M, Rim YS. On the nature of majority and minority traps in β-Ga_2O_3: A review. *Materials Today Physics.* 2023;36: 101155.
19. Spiridonov VA, Panov DI, Ivanov AY, Bauman DA, Romanov AE. The effect of high-temperature annealing on the properties of bulk β-Ga_2O_3 obtained in different growth atmospheres. *Materials Physics and Mechanics.* 2024;52(3): 80–85.
20. Kaminskii VV, Panov DYu, Spiridonov VA, Bauman DA, Kalganov DA, Scheglov MP, Romanov AE. Effect of high-temperature annealing on the internal friction and optical transmittance of single crystal gallium oxide. *Materials Physics and Mechanics.* 2024;52(5): 48–54.
21. Geller S. Crystal structure of β-Ga_2O_3. *The Journal of Chemical Physics.* 1960;33(3): 676–684.
22. Galeckas A, Cernescu A, Kaźmierczak-Bałata A, García-Fernández J, Bazioti C, Azarov A, Park JH, Jeon DW, Lee H, Lee WJ, Zhu R, Mei Z, Prytz O, Kuznetsov A. Optical library of Ga_2O_3 polymorphs. *arXiv.* Preprint posted online December 18, 2024;2412: 13987.
23. Víllora EG, Shimamura K, Yoshikawa Y, Aoki K, Ichinose N. Large-size β-Ga_2O_3 single crystals and wafers. *Journal of Crystal Growth.* 2004;270(3–4): 420–426.
24. Higashiwaki M. β-Ga_2O_3 material properties, growth technologies, and devices: a review. *AAPPS Bulletin.* 2022;32: 3.
25. Zhang K, Xu Z, Wang H, Zhang S, Dong B. Patterning the surface structure of transparent hard-brittle material β-Ga_2O_3 by ultrashort pulse laser. *Ceramics International.* 2022;48(19A):27650–27657.

26. Ahn M, Sarracino A, Ansari A, Torralva B, Yalisove S, Phillips J. Unique material modifications of Ga_2O_3 enabled by ultrafast laser irradiation. *Proceedings Volume 11281, Oxide-based Materials and Devices XI.* 2020;11281: 112810O.
27. Zhang K, Xu Z, Dong B, Zhang S. Process exploration of β-Ga_2O_3 blind hole processing by water-assisted femtosecond laser technology. *Journal of Alloys and Compounds.* 2023;939: 168769.
28. Panov DI, Spiridonov VA, Vasilev OS, Bogdanov PA, Bauman DA, Romanov AE. Laser processing of gallium oxide crystals in the preparation of samples for microelectronics. *Reviews on Advanced Materials and Technologies.* 2025;7(3): 198–202.
29. Yoo J, Rafique S, Lange A, Zhao H, Elhadj S. Lifetime laser damage performance of β-Ga_2O_3 for high power applications. *APL Materials.* 2018;6(3): 036105.
30. Zakgeim DA, Panov DI, Spiridonov VA, Kremleva AV, Smirnov AM, Bauman DA, Romanov AE, Odnoblyudov MA, Bougrov VE. Volume gallium oxide crystals grown from melt by the Czochralski method in an oxygen-containing atmosphere. *Technical Physics Letters.* 2020;46: 1144–1146.
31. Garcia-Lechuga M, Grojo D. Simple and robust method for determination of laser fluence thresholds for material modifications: An extension of Liu's approach to imperfect beams. *Open Research Europe.* 2021;1: 7.